Available online at www.derpharmachemica.com

ISSN 0975-413X
CODEN (USA): PCHHAX

Der Pharma Chemica, 2016, 8(18):186-203
(http://derpharmachemica.com/archive.html)

Quantum computational and vibrational spectroscopic analysis on Methyl 3-(2-(acetamidomethyl)-1-(phenylsulfonyl)indolin-3-yl)propanoate

R Srinivasaraghavan[a], S. Seshadri[b*] and T. Gnanasambandan[c]

[a]Department of Physics, SCSVMV University, Enathur, Kanchipuram 631 561, India
[b]Department of Physics, Dr. Ambedkar Govt. Arts college, Vyasarpadi, Chennai-39, India
[c]Department of Physics, Pallavan college of Engineering, Kanchipuram-631502, India

---

ABSTRACT

The complete vibration analysis of the fundamental modes of methyl 3-(2-(acetamidomethyl)-1-(phenylsulfonyl)indolin-3-yl)propanoate was carried out using the experimental FTIR and FT-Raman data and quantum chemical studies. The equilibrium geometry, harmonic vibrational wavenumbers of the compound were studied with the help of DFT method adopting 6-31G(d,p) and 6-311++G(d,p) basis sets. The theoretical results were interpreted with the IR and Raman spectral values. The value of Mulliken atomic charges, HOMO–LUMO energy gap were calculated. The intramolecular contacts were interpreted using natural bond orbital (NBO) and natural localized molecular orbital (NLMO) analysis to ascertain the charge distribution. The Molecular electrostatic potential studies were calculated for the compound to observe the electron densed region. Important non-linear properties such as electric dipole moment and first hyperpolarizability of the compound were computed using B3LYP quantum chemical calculations.

Keywords: M32A1PI3P, PED, NBO, NLMO, MEP

INTRODUCTION

The present investigation compound Methyl 3-(2-(acetamidomethyl)-1-(phenylsulfonyl)indolin-3-yl)propanoate [M32A1PI3P] is basically an indole derivative. Compounds containing the indole moiety exhibit antibacterial and fungicidal activities [1]. In addition indole derivatives are also known to exhibit anticancer and anti-HIV activities [2]. Some of the indole alkaloids extracted from lants possess interesting cytotoxic and antiparasitic properties [3,4]. The synthesis and geometrical parameters of the compound were studied by A.K. Mohanakrishnan et. al [5] based on similar type structure reported by Chakravarthi et. al [6,7]. After the process of synthesizing, studies related to vibrational spectroscopic investigation and assignments are not reported in the literature yet. Hence, in our present study, importance is given to the experimental and theoretical investigation of the vibrational and electronic transitions of M32A1PI3P. In the ground state theoretical geometrical parameters, IR and Raman spectra, HOMO and LUMO energies of title molecule were calculated by using Gaussian 03W program. Interpretations about the vibrational spectra of M32A1PI3P on the basis of the calculated potential energy distribution (PED) are given in detail. The experimental spectra are compared with the theoretically simulated spectral data; vibrational wavenumbers are in fairly good agreement with the experimental results. The redistribution of electron density (ED) in various bonding, antibonding orbitals and E (2) energies have been calculated by natural bond orbital (NBO) / Natural Localized Molecular Orbital (NLMO) analysis to give clear evidence of stabilization originating from the hyper conjugation of various intra-molecular interactions. The study of HOMO, LUMO analysis has been used to elucidate information regarding charge transfer within the molecule. Moreover, the Mulliken population analysis of the title compound are calculated and the results are reported. The experimental and theoretical results supported

each other, and the calculations are valuable for providing a reliable insight into the vibrational spectra and molecular properties.

MATERIALS AND METHODS

The compound Methyl 3-(2-(acetamidomethyl)-1-(phenylsulfonyl)indolin-3-yl)propanoate [M32A1PI3P] was a synthesized one reported in literature [5] and used as such without further purification to record FTIR and FT Raman spectra. The FTIR spectrum of the compound is recorded in the region 4000 – 400 cm^{-1} in evacuation mode on Bruker IFS 66V spectrophotometer using KBr pellet technique (solid phase) with 4.0 cm^{-1} resolutions. The FT-Raman spectra of these compounds are also recorded in the same instrument with FRA 106 Raman module equipped with Nd: YAG laser source operating at 1.064 μm line widths with 200 mW power. The spectra are recorded in the range of 3500–100 cm^{-1} with scanning speed of 30 cm^{-1} min^{-1} of spectral width 2 cm^{-1}. The frequencies of all sharp bands are accurate to ±1 cm^{-1}. The spectral measurements were carried out at Sophisticated Analytical Instrumentation Facility, IIT, Chennai, India.

COMPUTATIONAL DETAILS

A complete information regarding the structural characteristics and the fundamental vibrational modes of Methyl 3-(2-(acetamidomethyl)-1-(phenylsulfonyl)indolin-3-yl)propanoate [M32A1PI3P], has been carried out with the help of B3LYP correlation functional calculations using the Gaussian 03 W [8] program. DFT calculations were carried out with Becke's three-parameter hybrid model [9] using the Lee–Yang–Parr correlation [10] functional (B3LYP) method. The geometry optimization was carried out using the initial geometry generated from standard geometrical parameters of the B3LYP method with 6-31G (d, p) and 6-311++G (d, p) basis sets and the optimized geometry was determined by minimizing the energy with respect to all geometrical parameters without imposing molecular symmetry constraints. At the optimized structure of the examined species, no imaginary wavenumber modes were obtained, proving that a true minimum on the potential surface was found. The calculated frequencies are scaled according to the work of Rauhut and Pulay [9-10], a scaling factor of 0.9613 was used for both basis sets.

Scaling of the force field was performed according to the SQM procedure [11-12], using selective scaling in the natural internal coordinate representation. Transformation of force field, subsequent normal coordinates analysis and calculation of the Potential Energy Distribution (PED) were done on a PC with the MOLVIB program (version V7.0-G77) written by Sundius [13-15]. By the use of the GAUSSVIEW molecular visualization program [16] along with available literatural analysis of related molecules; the vibrational frequency assignments were made by their PED with a high degree of confidence.

RESULTS AND DISCUSSION

Molecular geometries

In order to find the most optimized geometry, the energies were carried out for M32A1PI3P, using B3LYP/6-311G(d,p) method and basis set for various possible conformers. Three conformers were obtained for M32A1PI3P and are shown in Figure 1. The total energies obtained for these conformers were 475.7708 kJ/mol; 4988.6744 kJ/mol and 489.6324 kJ/mol respectively. Of these three the first conformer shows minimum and therefore, C_1 form is the most stable conformer than the other conformers.

The optimized structure parameters calculated by DFT-B3LYP levels with the 6-31G(d,p) and 6-311++G(d,p) basis set are listed in the Table 1 in accordance with the atom numbering scheme given in Figure 2. Table 1 compares the calculated bond lengths and angles for M32A1PI3P with those experimentally available from literature value [5].

The theoretical values for the M32A1PI3P molecule were compared with the experimental values by means of the root mean square deviation values. Comparing the B3LYP/6-31G(d,p) and B3LYP/6-311++G(d,p) methods, most of the bond lengths and bond angles are the same in both the methods. The inclusion of diffusion and polarization functions is important to have a better agreement with experimental geometry.

Vibrational assignments

The molecular structure of M32A1PI3P belongs to C_1 point group symmetry and there would not be any relevant distribution for C_1 symmetry. The molecule M32A1PI3P consists of 49 atoms and expected to have 141 normal modes of vibrations of the same A species. These modes are found to be IR and Raman active, suggesting that the molecule possesses a non-centro symmetric structure.

The harmonic vibrational modes calculated for M32A1PI3P at B3LYP level using the 6-31G(d,p) and 6-311++G(d,p) basis set along with Potential energy distribution has been summarized in Tables 2 along with the experimental FTIR and FT Raman data. The experimental FT-IR and FT-Raman spectra with corresponding

theoretically simulated IR and Raman spectra of M32A1PI3P are shown in the Figures. 3 and 4 respectively, wherein the infrared and Raman intensities are plotted against the vibrational frequencies.

N-H vibrations

As solids or liquids, in which hydrogen bonding may occur, primary aliphatic amines absorb in the region 3480 – 3250 cm^{-1} [17]. This is a broad band of medium intensity which may show structure depending on the hydrogen bond polymers formed. In dilute solution of non-polar solvents, two bands are observed for primary amines and may be due to the N-H asymmetric and symmetric vibrations. In aliphatic case, they are in the range 3500 – 3250 cm^{-1} whereas in aromatic case they occupy the same region but with medium intensity. Secondary amines have only one N-H stretching band which is usually weak and occurs in the range of 3500 – 3300 cm^{-1}. In solid and liquid phases, a band of medium intensity may be observed at 3400 – 3300 cm^{-1} for secondary aromatic amines. Arjunan et al [18] have identified N-H vibrations in the region of 3350 cm^{-1}. Muthu et al [19] identified N-H vibration to be in the region 3430cm^{-1}, Based on the above reference, In the present investigation, the band appear at 3473 cm^{-1} is assigned to N-H stretching mode of vibration. The theoretically calculated modes match with the experimentally observed values of same mode.

Primary amines have a medium to strong absorption in the region 1650 – 1580 cm^{-1} due to amine N-H deformation vibrations. The medium band present at 1583 cm^{-1} in the FTIR spectrum is considered to be due to N-H deformation. Secondary aliphatic amines have an absorption in the range 850 – 750 cm^{-1} due to N-H deformation. Based on the above, the band observed at 857 cm^{-1} in the FTIR spectrum is assigned to be due to C-N-H deformation.

C-H Vibrations

The benzene derivatives give rise to C H stretching, C H in-plane and C H out-of-plane bending vibrations. Aromatic compounds commonly exhibit multiple weak bands in the region 3200–3000 cm^{-1} due to C-H stretching bands. [20] due to aromatic C H stretching vibrations. The in plane bending of C-H vibrations occupy the region between 1400-1100 cm^{-1}. Similarly the out of plane modes may occur between 800-1100 cm^{-1} [21,22]. In this region, the vibrations are not found to be affected due to the nature and position of the substituent [23]. Based on the above observations, in our present study, the bands observed at 3198, 3190, 3181 and 3177 cm^{-1} are assigned to C-H asymmetric vibrations and 3159, 3144, 3080, 3067 cm^{-1} in the M32A1PI3P compound have been assigned to C-H symmetric stretching vibration. Apart from the mentioned values other vibrations in the same range are assigned to C-H stretching vibrations respectively. The C-H bending vibrations appear at two distinct regions 1480 - 1100 cm^{-1} and 1100 – 900 cm^{-1}, ant these regional vibrations due to in plane and out of plane bending C-H vibrations are very useful for characterization purpose [24,25]. The band position observed at 1480 and at 1428 cm^{-1} in the spectra of M32A1PI3P are assigned to C-H in plane bending vibrations. The strong peaks below 1000 cm^{-1}, clearly indicate its aromaticity. Substitution patterns on the ring can be judged from the out-of-plane bending of the ring C–H bonds in the region 900–675 cm^{-1} and these bands are highly informative [22]. Monosubstituted benzene shows only a strong band between 700 and 770 cm^{-1} [23]. In our present study, the band at 996, 962, 810 and 721 cm^{-1} in the FTIR and FT Raman spectra confirms the presence of C-H out of plane bending vibrations of this compound. The wave numbers calculated through DFT techniques are in good agreement with the experimental data [26].

C-N Stretching

Silverstien et al [27] assigned C-N stretching absorption in the region 1342 cm^{-1} - 1266 cm^{-1}. The spectra of benzene and pyridyl substituted compounds exhibit the band in the region 1260 – 1210 cm^{-1}. In vibrational analysis of some pyrazole derivatives, Chitambarathanu et al [28] have identified C-N stretching vibrations at 1292, 1290, 1284 cm^{-1} in FTIR spectra. Gunasekaran et al [29] has identified the C-N stretching vibrations at 1310, 1287 and 1230 cm^{-1} in the vibrational analysis of Aminophylline. In analogy with the previous works, the bands appear at 1386, 1353 and 1297 cm^{-1} in the experimental analysis spectrum of M32A1PI3P are assigned to C-N stretching vibration.

C-C vibrations

In most of the mononuclear and polynuclear aromatic compounds, the ring C-C stretching vibrations occur in the region 1625-1530 cm^{-1} [30]. According to Bellamy, the actual positions are determined not so much by the nature of the substituents, but rather by the form of the substitution around the ring [31]. Mohan et al [32] have reported that the IR band observed at 1480 and 1465 cm^{-1} in the vibrational analysis of 2-aminopyrimidine due to C-C vibrations. Singh et al [33] have identified the FTIR bands at 1576, 1504, and 1468 cm^{-1} in pyrazzole derivatives due to aromatic C-C stretching vibrations. Hence in the present investigation, the wavenumber appear at 1485, 1423 and 1400 cm^{-1} in the FTIR and FT Raman spectra of M32A1PI3P are assigned to C-C stretching mode of vibrations. The DFT theoretical study results match and are in agreement with the experimentally observed ones.

C=O vibration
Ketones absorb strongly in the range 1650 – 1550 cm^{-1} and in solids, the frequency of C=O stretching vibration is 10-20 cm^{-1} lower than that observed in dilute solutions with non – polar solvents. Aryl ketones absorb in the region 1700-1600 cm^{-1} [34]. In the present compound the band at 1632 cm^{-1} is assigned to C=O stretching vibration.

C-S Vibration
In general, the assignment of the band due to C-S stretching vibrations in different compounds is difficult. Both aliphatic and aromatic sulphides have weak to medium band due to C-S stretching especially in the region 780 - 510 cm^{-1} [35,36]. Double bond conjugation with the C-S band like vinyl or phenyl lowers the C-S stretching frequency and increases the intensity. In view of this, the medium intensed bands present at 581 and 769 cm^{-1} in the FTIR spectrum of M32A1PI3P and the band at 769 cm^{-1} in the FT Raman spectrum of M32A1PI3P are assigned to be due to C-S stretching modes of vibration.

S =O Stretching vibration
In solid phase sulphonamides have a strong, broad absorption band at 1360-1315 cm^{-1} due to the asymmetric stretching vibration of S=O group, whereas the symmetric stretching vibration of this group shows the occurrence at 1280 - 1240 cm^{-1} [37,38]. Similarly, in the case of dilute solutions in nonpolar solvents, all organic sulphonamides have two strong bands at 1360 – 1290 cm^{-1} and 1270-1220 cm^{-1} due to asymmetric and symmetric stretching vibrations respectively. In the present case, the FTIR spectrum of M32A1PI3P, shows the presence of the bands due to symmetric and asymmetric stretching of S=O group at 1229 cm^{-1} and at 1297 cm^{-1} respectively.

RESULTS AND DISCUSSION

Method of calculations
All calculations were performed with Gaussion 03W software with two different basis sets of DFT. In addition to geometry optimization and vibrational spectra, B3LYP results were also used to obtain NLO properties, polarisabilities, energies (E_{HOMO}, E_{LUMO} and $\Delta E = E_{LUMO}-E_{HOMO}$) and other quantum chemical parameters of M32A1PI3P.

The energy of an uncharged molecule under a general electric field can have terms related to μ_I, α_{ij}, β_{ijk} are the dipole moment, the polarisibility and the first order hyper polarisibility respectively. Based on that the ground state dipole moment (μ), the polarisibility (α) and the anisotropy of the polarisibility ($\Delta\alpha$) are defined as

$$\mu = [\mu^2_x + \mu^2_y + \mu^2_z]^{1/2}$$

$$\alpha = \frac{\alpha xx + \alpha yy + \alpha zz}{3}$$

$$\Delta\alpha = 2^{-1/2} [(\alpha_{xx} - \alpha_{yy})^2 + (\alpha_{yy} - \alpha_{zz})^2 + (\alpha_{zz} - \alpha_{xx})^2 + 6\, \alpha^2_{xx}]^{1/2}$$

The first order hyperpolarizability (β_0) is a third rank tensor that can be described by 3 x 3 x 3 matrix. The 27 components of the matrix can be reduced to 10 components due to Kleinman symmetry [39]. The components of the first order hyperpolarisibility can be calculated using the following relations

$$\beta = [\beta^2_x + \beta^2_y + \beta^2_z]^{1/2}$$

Where $\beta_x = \beta_{xxx} + \beta_{xyy} + \beta_{xzz}$
$\beta_y = \beta_{yyy} + \beta_{xxy} + \beta_{yzz}$
$\beta_z = \beta_{zzz} + \beta_{xxz} + \beta_{yyz}$

The E_{HOMO} and E_{LUMO} are used to approximate the ionization potential (I) and electron affinity (A) given by Koopman's theorem [40]. $I = -E_{HOMO}$ and $A=-E_{LUMO}$. It is assumed that these relations are valid within the DFT frame. The electronetagivity, hadrness and chemical potential can be estimated with the formula

$$\eta = \frac{I-A}{2} \qquad \mu = \frac{-(I+A)}{2} \qquad \chi = \frac{I+A}{2}$$

The softness (σ) is also given by $\sigma = 1/\eta$ [41]

Electric moments and NLO properties
Analysis of organic compounds having conjugated π- electron systems and large hyperpolarisability using IR and Raman spectroscopy has evolved as a subject of research [42,43]. The prime application of the compound in the

field of non linear optics demands investigation of its structural bonding features contributing to the hyperpolarisability, enhancement by analyzing the vibrational modes using IR and Raman spectroscopy. The method B3LYP/6-311++G(d,p) has been used for the prediction of first order hyperpolarizability (β) of the title compound and the values are shown in Table 3. The calculated value of first hyperpolarizability shows that M32A1PI3P might have the NLO properties. The nonlinear optical activity provides useful information for frequency shifting, optical modulation, optical switching and optical logic for the developing technologies in areas such as communication, signal processing and optical interconnections.

Electronic properties

The Highest Occupied Molecular Orbitals (HOMOs) and Lowest–Lying Unoccupied Molecular Orbitals (LUMOs) and the energy gap between the HOMOs and LUMOs is the critical parameters in determining molecular electrical transport properties that helps in the measure of electron conductivity. To understand the bonding feature of the title molecule, the plot of the Frontier orbitals, the HOMO and LUMO is shown in Figure 5. The HOMO shows that the charge density localized mainly on carbonyl and amine group where as LUMO is localized on ring system. The group contribution to the molecular orbitals and in turn helps for preparing the density of state (DOS) diagram is shown in Figure 6.

The ionization potential calculated by B3LYP/6-31G(d,p) and B3LYP/6-311++G(d,p) methods for M32A1PI3P is 7.8119 eV and 4.6017 eV respectively. Considering the chemical hardness, large HOMO–LUMO gap means a hard molecule and small HOMO–LUMO gap means a soft molecule. One can also relate the stability of the molecule to hardness, which means that the molecule with least HOMO–LUMO gap means it, is more reactive. Parr et al. [43] have proposed electrophilicity index (ω) as a measure of energy, lowering due to maximal electron flow between donor and acceptor. They defined electrophilicity index (x) as follows:

$$\omega = \frac{\mu^2}{2}$$

Using the above equations, the chemical potential, hardness and electrophilicity index have been calculated for M32A1PI3P and their values are shown in Table 4. The usefulness of this new reactivity quantity has been recently demonstrated in understanding the toxicity of various pollutants in terms of their reactivity and site selectivity [44-46]. The calculated value of electrophilicity index describes the biological activity of M32A1PI3P.

NBO/ NLMO analysis

NBO analysis has been performed on M32A1PI3P in order to elucidate intramolecular hydrogen bonding, intramolecular charge transfer (ICT) interactions and delocalization of π-electrons. By the use of the second-order bond–antibond (donor–acceptor) NBO energetic analysis, insight in the most important delocalization schemes were obtained. The change in electron density (ED) in the (σ*, π*) antibonding orbitals and E(2) energies have been calculated by natural bond orbital (NBO) analysis [47] using DFT methods to give clear evidence of stabilization originating from various molecular interactions. The hyperconjugative interaction energy was deduced from the second-order perturbation approach [48].

$$E(2) = - \frac{(\sigma| F| \sigma)^2}{\varepsilon \sigma' - \varepsilon \sigma} n_\sigma \qquad \frac{F_{ij}^2}{\Delta E} -n_\sigma$$

Where $(\sigma|F|\sigma)^2$ or F_{ij}^2 is the Fock matrix element between the i and j NBOs, ε_σ and ε_{σ^*} are the energies of σ and σ* NBOs, and n_σ is the population of the donor σ orbital.

In Table 5, the perturbation energies of significant donor–acceptor interactions are presented. The larger the E(2) value, the intensive is the interaction between electron donors and electron acceptors. In M32A1PI3P, the interactions between the first lone pair of nitrogen N_{28} and the antibonding of C_{25} - O_{27}have the highest E(2) value around 52.67 kcal/mol. The other significant interactions giving stronger stabilization energy value of 47.60 kcal/mol to the structure are the interactions between antibonding of C_{25}- O_{27}between the second lone pair of oxygen O_5.

Table 5 gives the occupancy of electrons and p-character [49] in significant NBO natural atomic hybrid orbital. In C–H bonds, the hydrogen atoms have almost 0% of p-character. The 100% p-character is observed in the first lone pair of N_6 and in the second lone pair of O_4, O_5 and $O_{27}$and in the third lone pair of $O_{16}$and O_{17}.

The natural localized molecular orbital (NLMO) analysis has been carried out since they show how bonding in a molecule is composed from orbitals localized on different atoms. The derivation of NLMOs from NBOs gives direct insight into the nature of the localized molecular orbital's ''delocalization tails'' [50, 51]. Table 5 shows significant NLMO's occupancy, percentage from parent NBO and atomic hybrid contributions of M32A1PI3P calculated at B3LYP level using 6-311++G (d,p) basis set. The NLMO of first lone pair of nitrogen atom N6 is the most delocalized NLMO and has only 82.094% contribution from the localized LP(1) N6 parent NBO, and the delocalization tail (~13.74%) consists of the hybrids of C_7,and C8.

Molecular electrostatic potential

Molecular electrostatic potential is a very useful quantity to illustrate the charge distributions of molecule and is used to visualize variably charged regions of a molecule [52]. The molecular electrostatic potential is widely used as a reactivity map displaying most probable regions for the electrophilic attack of charged point-like reagents and also for the analysis of molecular structure with its physiochemical property relationship on organic molecules [53]. The different values of the electrostatic potential are represented by different colors. So potential increases in the order: red < orange < yellow < green < cyan < blue. Therefore red indicates negative regions, blue indicates positive regions, while green appears over zero electrostatic potential regions. The use of a symmetrical potential scale values eases the recognition of positive, zero or negative regions.

A 3D plot of the molecular electrostatic potential map of M32A1PI3P calculated at B3LYP/6-311++G (d,p) optimized geometries is shown in Figure 7. The total energy distribution plot of the compound shows uniformity in distribution. However, it is observed from the diagram that the negative MEP is localized more over oxygen and nitrogen atoms in the compound and are reflected by yellow shades of colour. The regions having positive potential are over all hydrogen atoms. According to the calculated results, the MEP shows negative potential sites more on nitrogen and oxygen atoms indicating strongest repulsion over these regions, while the positive potential sites around the hydrogen atoms indicating strongest attraction over these potential regions. The negative regions of potential were related to electrophilic reactivity and the positive ones to nucleophilic reactivity [54].

It can be seen that the most possible sites for electrophilic attack is H15. Negative regions of the studied molecule are found around the O4, C1, C9, C10 and C11 atoms indicating a possible site for nucleophilic attack. According to these calculated results, the MEP map shows that the negative potential sites are on electronegative atoms as well as the positive potential sites are around the hydrogen atoms.

Mulliken Charge distribution

It is clear that Mulliken population analysis yield one of the simplest pictures of charge distribution and Mulliken charges render net atomic population in the molecule. The charge distribution of the compound have been calculated using the DFT method B3LYP/6-311++G(d,p) level of theory and is shonw in Figure 8. The Mulliken atomic charge distribution results are tabulated in Table 6. From table 6, it is clearly seen that the magnitude of carbon atomic charges found to be either positive or negative, were noted with the range of values. All the hydeogen atoms and sulphur atoms possess positive charge whereas the nitrogen atoms has a negative charge.

Temperature dependence of thermodynamic properties

The values of thermodynamic parameters such as heat capacity, entropy and enthalpy were calculated using perl script THERMO.PL [55] and are listed in Table 7. As observed from the Table, the values of C_P, H and S all increase with the increase of temperature from 100 to 1000 K, which is attributed to the enhancement of the molecular vibration as the temperature increases. The correlation equations between heat capacity ($C^\circ pm$), entropy(S°_m), enthalpy (H°_m) changes and temperatures were fitted by quadratic formulas and the corresponding fitting factors (R^2) for these thermodynamic properties are 0.9999, 0.9998 and 0.9998, respectively. The corresponding fitting equations are as follows and the correlation graphs of those shown in Figure 9.

$$S^o m = 240.03433 + 0.7328\ T - 1.79433\times10^{-4}\ T^2\ (R^2 = 0.9999)$$
$$C^o pm = 15.26587 + 0.65639\ T - 2.82786\times10^{-4}\ T^2\ (R^2 = 0.9998)$$
$$H^o_m = -7.65942 + 0.08696\ T + 1.73344\times10^{-4}\ T^2\ (R^2 = 0.9998)$$

All the thermodynamic data provide helpful information to further study of the title compounds. They compute the other thermodynamic energies according to the relationship of thermodynamic functions and estimate directions of chemical reactions according to the second law of thermodynamics in thermo chemical field.

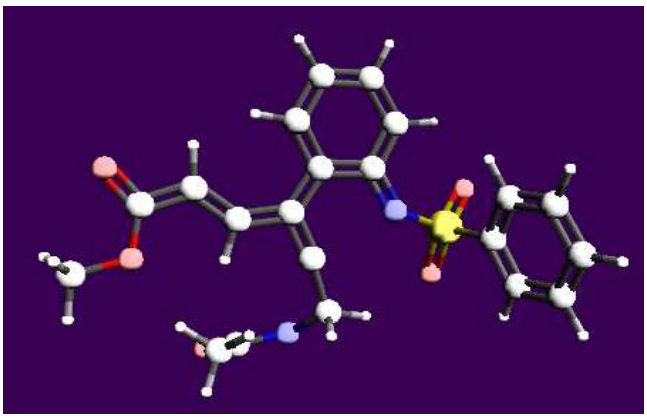

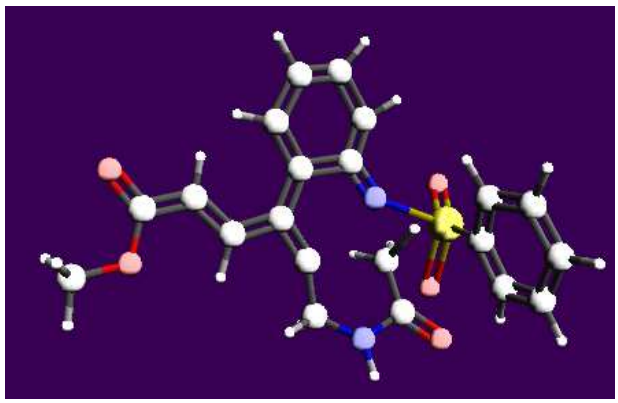

C1= 475.7708 kJ/mol C2=4988.6744 kJ/mol

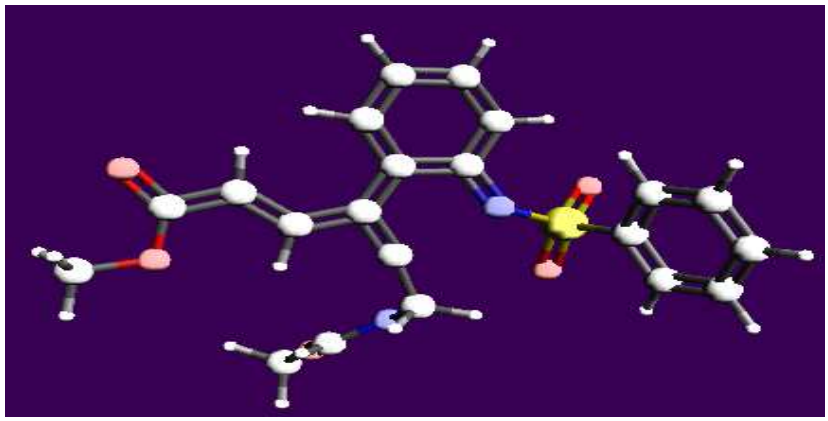

C3= 489.6324 kJ/mol

Figure 1 Conformer structure of Methyl 3-(2-(acetamidomethyl)-1-(phenylsulfonyl)indolin-3-yl)propanoate

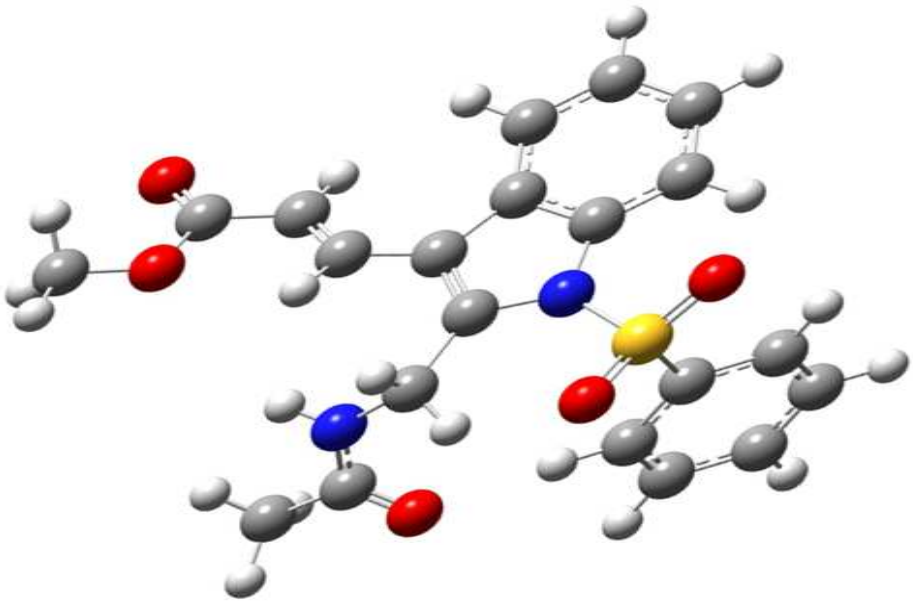

Figure 2. Optimised Structure of M32A1PI3P

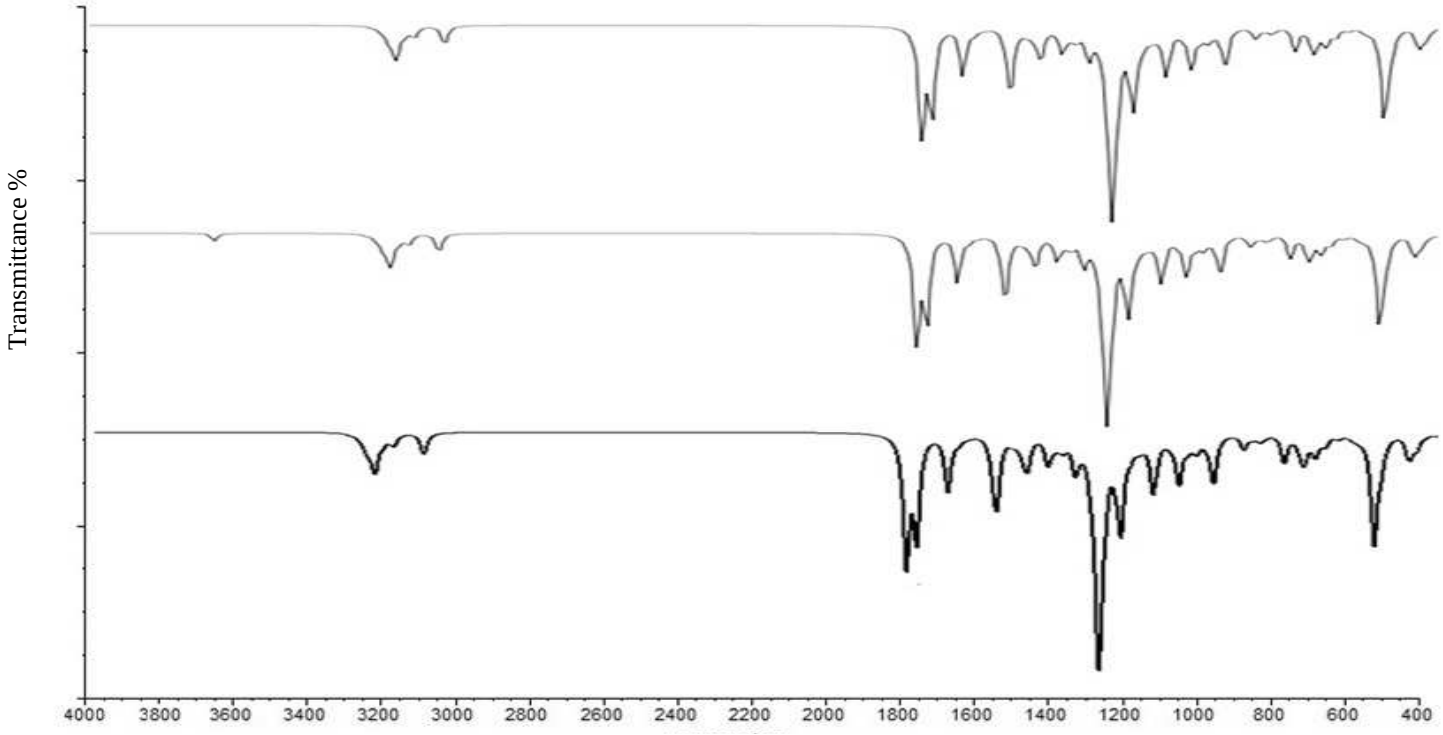

Figure 3 Comparative Experimental and Theoretical IR spectra of M32A1PI3P

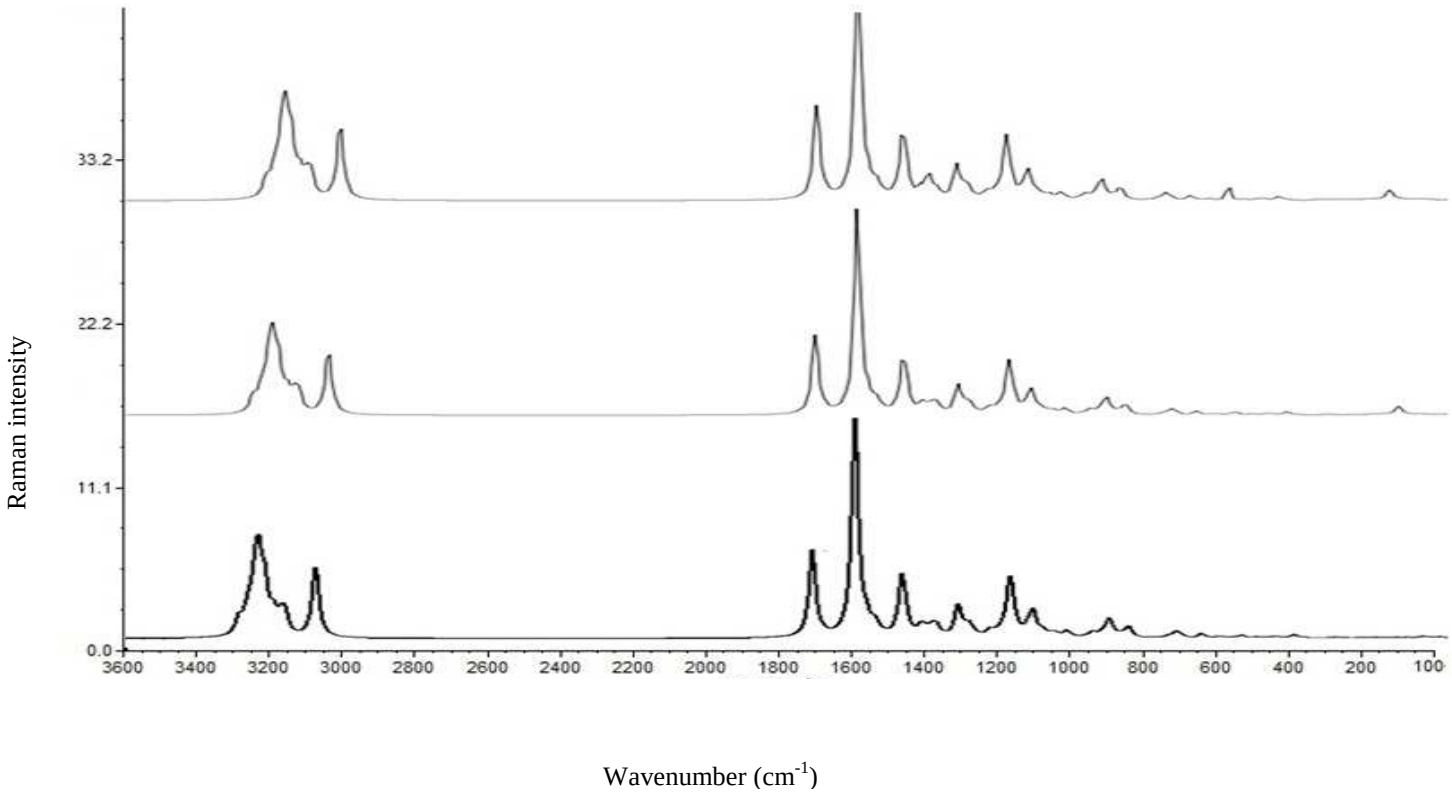

Figure 4 Comparative Experimental and Theoretical Raman spectra of M32A1PI3P

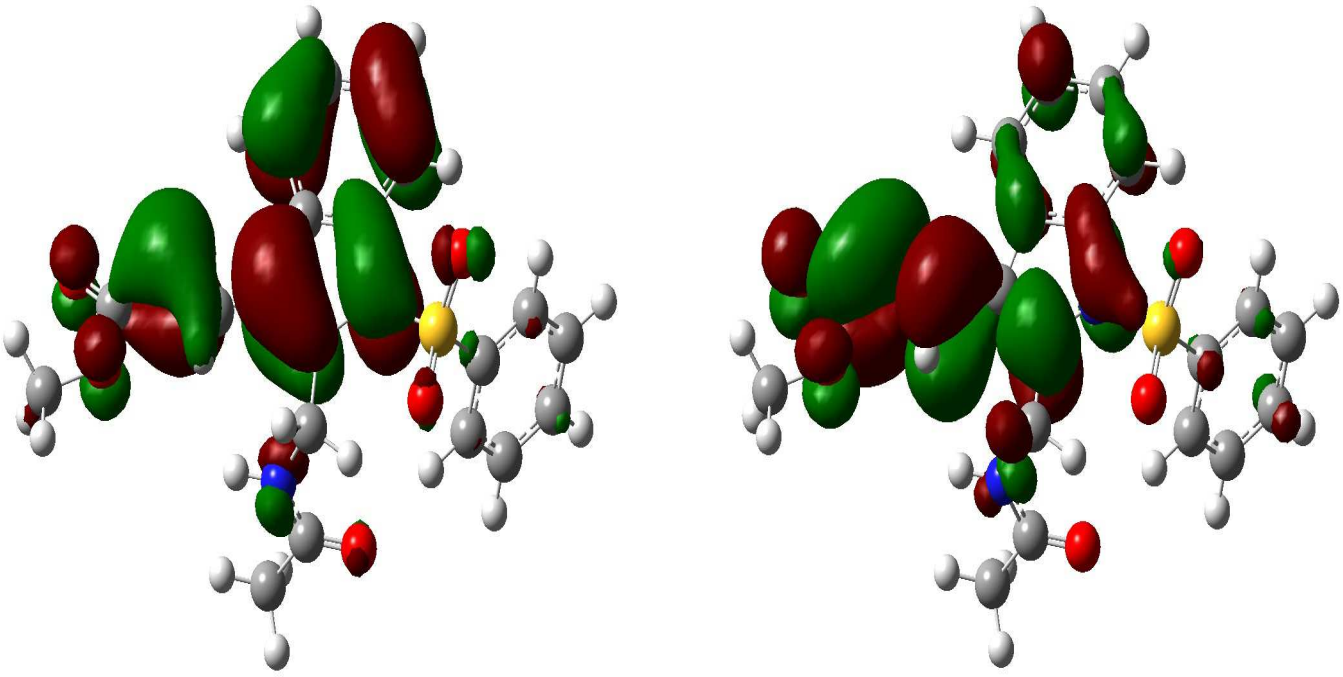

HOMO DIAGRAM **LUMO DIAGRAM**

Figure 5 Frontier molecular orbital M32A1PI3P

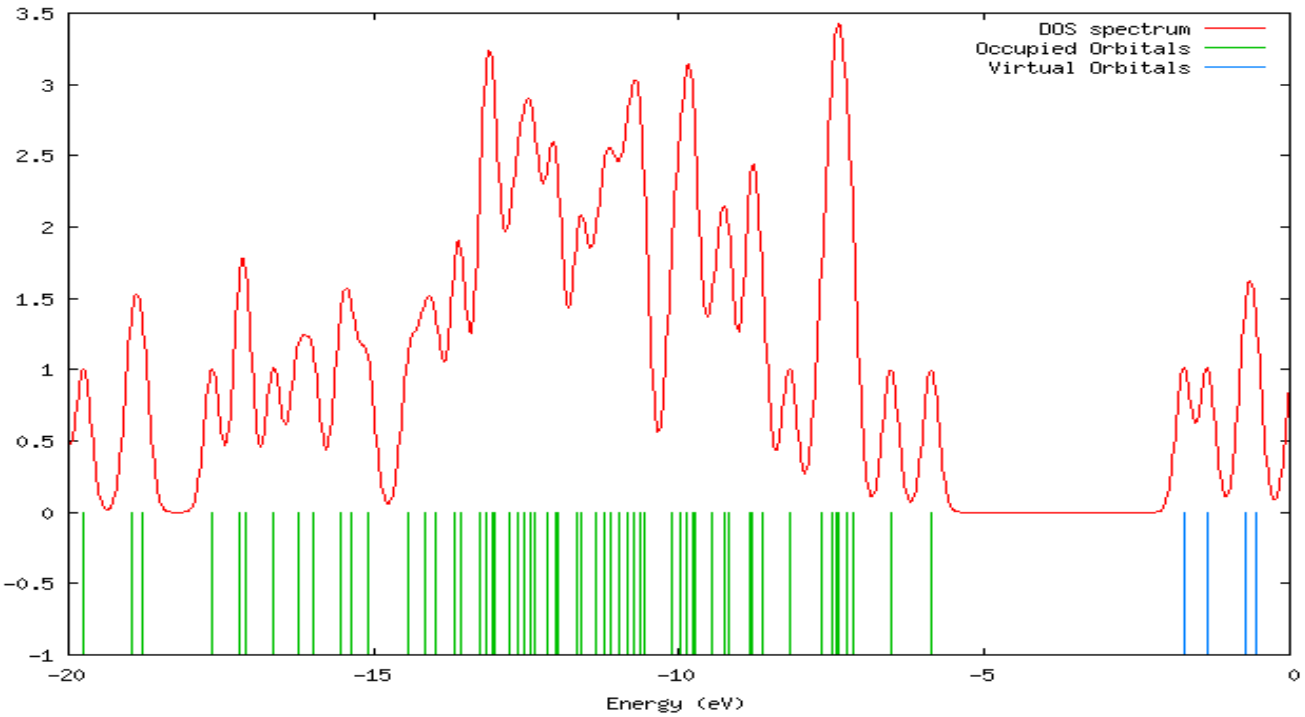

Figure 6 DOS spectrum of M32A1PI3P

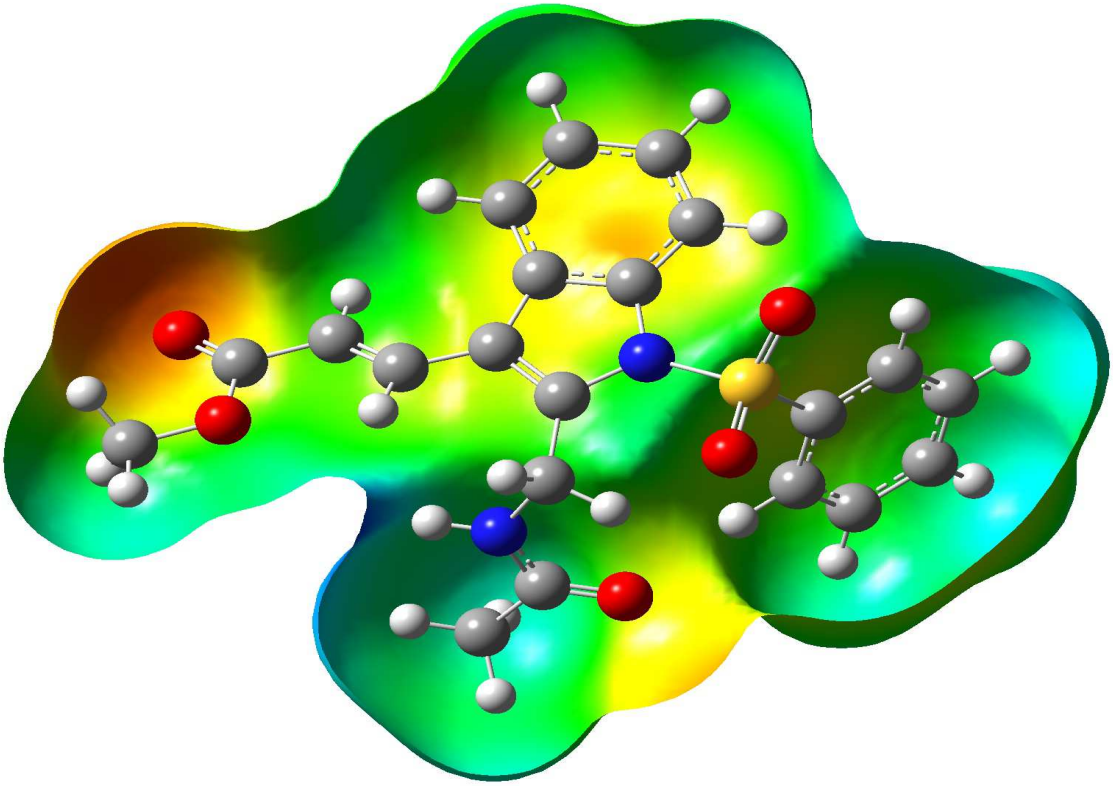

Figure 7 Molecular electrostatic potential of M32A1PI3P

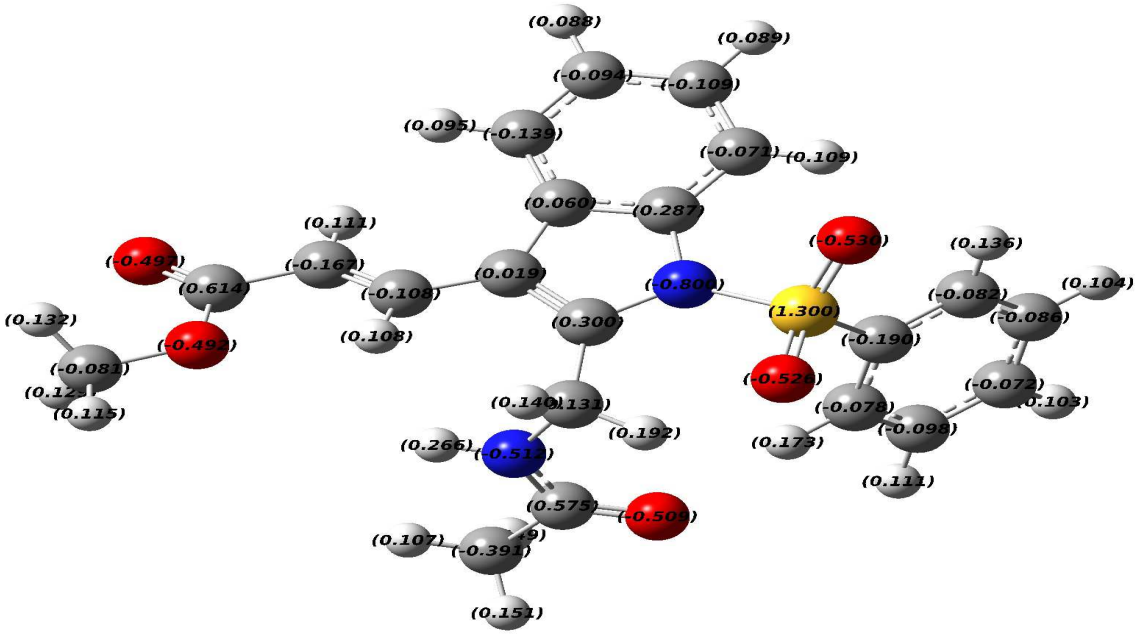

Figure 8 Mulliken atomic charge distribution of M32A1PI3P

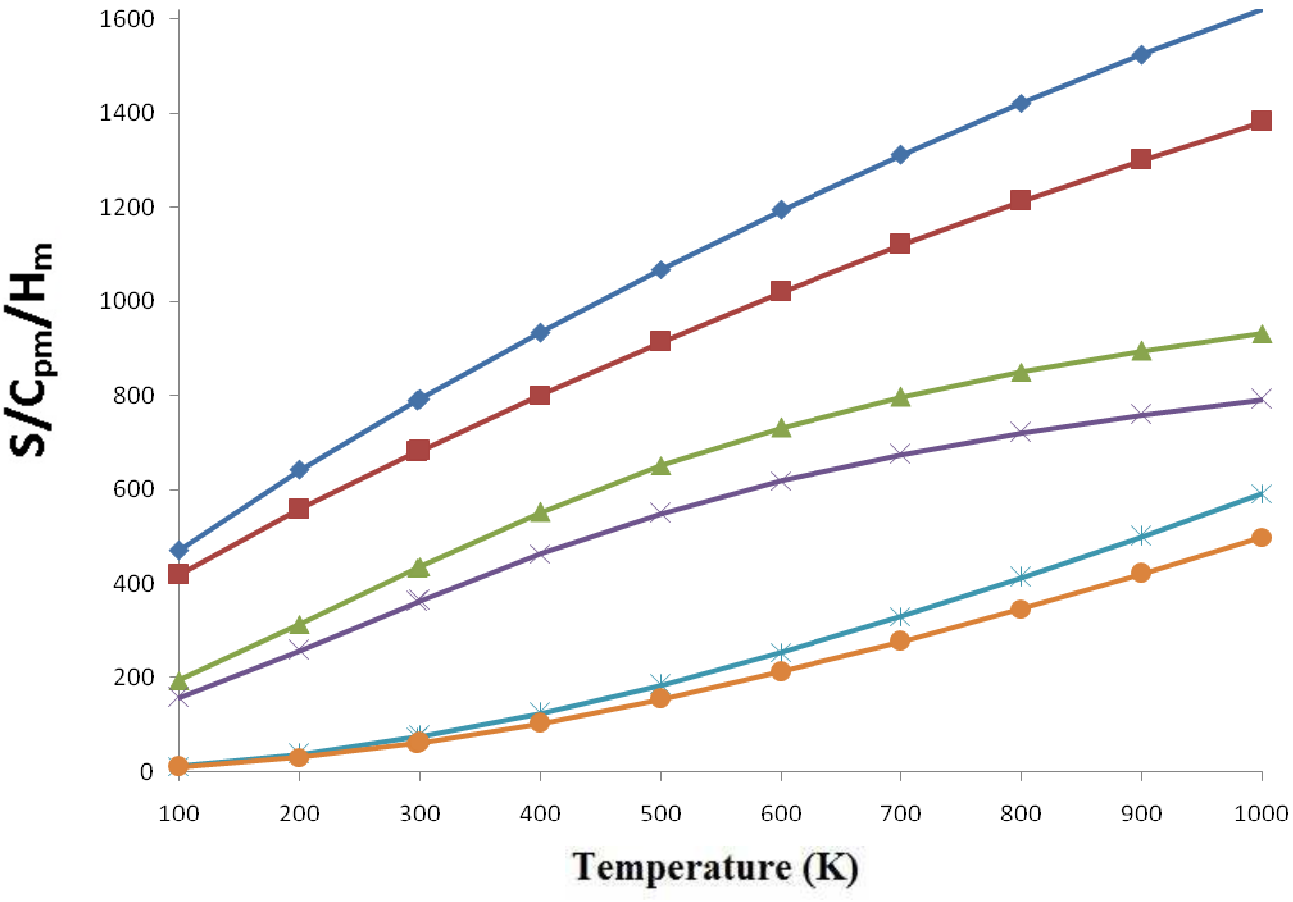

Figure 9 Thermodynamical properties of M32A1PI3P by B3LYP/6-31G(d,p) and B3LYP/6-311++G(d,p)

Table 1 Molecular parameters of M32A1PI3P

Molecular parameters	expt	6-31G(d,p)	6-311++G(d,p)
H(49)-C(29)	1.11	1.11	1.09
H(48)-C(29)	1.11	1.11	1.09
H(47)-C(29)	1.11	1.11	1.09
H(46)-N(28)	1.01	0.99	1.00
H(45)-C(26)	1.11	1.11	1.09
H(44)-C(26)	1.11	1.11	1.09
H(43)-C(26)	1.11	1.11	1.09
H(42)-C(24)	1.11	1.13	1.09
H(41)-C(24)	1.11	1.12	1.08
H(40)-C(23)	1.10	1.10	1.08
H(39)-C(22)	1.10	1.10	1.08
H(38)-C(21)	1.10	1.10	1.08
H(37)-C(20)	1.10	1.10	1.08
H(36)-C(19)	1.10	1.10	1.08
H(35)-C(13)	1.10	1.10	1.08
H(34)-C(12)	1.10	1.10	1.08
H(33)-C(11)	1.10	1.10	1.08
H(32)-C(10)	1.10	1.10	1.08
H(31)-C(3)	1.10	1.10	1.10
H(30)-C(2)	1.10	1.10	1.08
C(29)-O(5)	1.40	1.41	1.40
N(28)-C(25)	1.36	1.39	1.36
N(28)-C(24)	1.45	1.43	1.46
O(27)-C(25)	1.20	1.24	1.22
C(26)-C(25)	1.50	1.50	1.51
C(24)-C(7)	1.49	1.50	1.51
C(23)-C(18)	1.33	1.40	1.39
C(23)-C(22)	1.33	1.39	1.39
C(22)-C(21)	1.33	1.39	1.39
C(21)-C(20)	1.33	1.39	1.39
C(20)-C(19)	1.33	1.39	1.39
C(19)-C(18)	1.33	1.40	1.39

C(18)-S(15)	1.79	1.68	1.79
O(17)-S(15)	1.45	1.40	1.45
O(16)-S(15)	1.45	1.39	1.45
S(15)-N(6)	1.69	1.69	1.69
C(14)-N(6)	1.26	1.42	1.41
C(14)-C(13)	1.33	1.40	1.39
C(14)-C(9)	1.33	1.44	1.41
C(13)-C(12)	1.33	1.38	1.39
C(12)-C(11)	1.33	1.40	1.40
C(11)-C(10)	1.33	1.39	1.38
C(10)-C(9)	1.33	1.39	1.40
C(9)-C(8)	1.33	1.45	1.44
C(8)-C(7)	1.33	1.40	1.38
C(8)-C(3)	1.33	1.43	1.44
C7-C6	1.32	1.41	1.40
O(5)-C(1)	1.33	1.37	1.36
O(4)-C(1)	1.20	1.23	1.21
C(3)-C(2)	1.33	1.34	1.34
C(2)-C(1)	1.35	1.46	1.47
O(5)-C(29)-H(47)	109.50	103.70	105.70
O(5)-C(29)-H(48)	109.44	110.00	110.80
O(5)-C(29)-H(49)	109.46	109.90	110.70
H(47)-C(29)-H(48)	109.44	111.50	110.50
H(47)-C(29)-H(49)	109.46	111.50	110.40
H(48)-C(29)-H(49)	109.52	110.00	108.60
C(24)-N(28)-C(25)	120.00	121.20	120.70
C(24)-N(28)-H(46)	120.00	118.80	119.20
C(25)-N(28)-H(46)	120.00	117.40	118.30
C(25)-C(26)-H(43)	109.50	110.50	110.10
C(25)-C(26)-H(44)	109.44	110.40	108.70
C(25)-C(26)-H(45)	109.46	108.70	108.50
H(43)-C(26)-H(44)	109.44	109.20	108.90
H(43)-C(26)-H(45)	109.46	109.00	109.20
H(44)-C(26)-H(45)	109.52	109.00	107.40
C(26)-C(25)-O(27)	120.00	121.90	121.40
C(26)-C(25)-N(28)	120.00	118.20	118.50
O(27)-C(25)-N(28)	120.00	120.90	120.10
C(7)-C(24)-N(28)	109.50	113.60	113.50
C(7)-C(24)-H(41)	109.44	109.40	110.30
C(7)-C(24)-H(42)	109.46	110.50	109.10
N(28)-C(24)-H(41)	109.44	109.20	109.20
N(28)-C(24)-H(42)	109.46	109.80	109.40
H(41)-C(24)-H(42)	109.52	109.20	109.00
H(40)-C(23)-C(18)	120.00	119.20	120.00
H(40)-C(23)-C(22)	120.00	120.90	119.60
C(18)-C(23)-C(22)	120.00	119.20	120.00
H(39)-C(22)-C(23)	120.00	120.10	120.30
H(39)-C(22)-C(21)	120.00	120.00	119.60
C(23)-C(22)-C(21)	120.00	119.90	120.00
H(38)-C(21)-C(22)	120.00	119.90	120.40
H(38)-C(21)-C(20)	120.00	120.00	119.80
C(22)-C(21)-C(20)	120.00	120.10	119.80
H(37)-C(20)-C(21)	120.00	120.00	119.10
H(37)-C(20)-C(19)	120.00	120.10	120.40
C(21)-C(20)-C(19)	120.00	119.80	120.50
H(36)-C(19)-C(20)	120.00	121.00	119.20
H(36)-C(19)-C(18)	120.00	119.30	120.60
C(20)-C(19)-C(18)	120.00	119.30	120.50
S(15)-C(18)-C(23)	120.00	120.70	119.40
S(15)-C(18)-C(19)	120.00	120.80	119.30
C(23)-C(18)-C(19)	120.00	118.40	120.30
O(16)-S(15)-O(17)	119.50	119.20	119.30
O(16)-S(15)-N(6)	109.44	110.80	109.90
O(16)-S(15)-C(18)	109.46	110.30	109.80
O(17)-S(15)-N(6)	109.44	110.40	109.90
O(17)-S(15)-C(18)	109.46	107.30	110.10
N(6)-S(15)-C(18)	109.52	110.30	109.80
N(6)-C(14)-C(13)	118.99	119.70	119.20
N(6)-C(14)-C(9)	117.00	118.30	118.10
C(13)-C(14)-C(9)	119.99	120.10	119.90
H(35)-C(13)-C(14)	120.00	119.60	119.60
H(35)-C(13)-C(12)	120.00	119.20	119.60
C(14)-C(13)-C(12)	120.00	121.50	121.40
H(34)-C(12)-C(13)	120.00	119.30	119.60
H(34)-C(12)-C(11)	120.00	119.20	119.00

C(13)-C(12)-C(11)	119.99	118.00	119.60
H(33)-C(11)-C(12)	120.00	120.90	120.70
H(33)-C(11)-C(10)	120.00	121.10	120.80
C(12)-C(11)-C(10)	119.91	120.20	119.50
H(32)-C(10)-C(11)	120.00	119.60	119.80
H(32)-C(10)-C(9)	120.00	119.70	119.20
C(11)-C(10)-C(9)	120.00	118.90	119.10
C(8)-C(9)-C(14)	119.00	120.70	120.70
C(8)-C(9)-C(10)	119.99	120.80	120.00
C(14)-C(9)-C(10)	119.99	120.40	120.20
C(3)-C(8)-C(7)	120.50	121.10	120.80
C(3)-C(8)-C(9)	120.50	120.80	120.00
C(7)-C(8)-C(9)	119.00	120.40	120.20
C(8)-C(7)-C(24)	119.48	121.10	120.80
C(14)-N(6)-S(15)	117.01	119.60	119.60
C(1)-O(5)-C(29)	120.00	119.20	119.60
C(2)-C(3)-C(8)	120.00	121.50	121.40
C(2)-C(3)-H(31)	120.00	119.30	119.60
C(8)-C(3)-H(31)	120.00	119.20	119.00
C(1)-C(2)-C(3)	120.00	119.60	119.60
C(1)-C(2)-H(30)	120.00	118.50	120.80
C(3)-C(2)-H(30)	120.00	119.50	119.90
C(2)-C(1)-O(4)	120.00	120.10	120.60
C(2)-C(1)-O(5)	120.00	120.50	120.70
O(4)-C(1)-O(5)	120.00	119.30	119.20

Table 2 Vibrational assignments of M32A1PI3P using B3LYP/ 6-31 G(d,p) and B3LYP/6-311++G(d,p)

νIR cm^{-1}	ν Raman cm^{-1}	B3LYP/6-31 G(d,p)			B3LYP/6-311++ G(d,p)			Assignments with PED (%)
		ν cm^{-1}	IR Intensity	Raman	ν cm^{-1}	IR Intensity	Raman	
		14	0.6856	4.2042	14	1.2911	1.1989	τ ring (12)
		16	2.7119	6.8439	17	4.8341	0.8362	β ring (19)
		29	0.4361	1.3563	28	3.4879	1.4301	τCN (18)
		36	1.7035	1.1705	37	0.185	2.75	γSO_2(wag) (22)
		46	3.0167	5.206	46	0.9534	1.2966	τ ring (15)
		54	0.5985	2.2251	54	0.5986	0.1645	Ring sci. (17)
		57	0.9319	2.4411	58	1.3917	0.0798	βring (17)
		64	0.9908	4.208	65	1.0808	6.8735	γCH_3(wag) (12)
		73	0.9698	1.4327	74	0.2725	0.4364	γSO_2(wag) (18)
		87	0.2184	0.6153	87	3.0082	2.5003	γCC(72)
		98	9.5611	3.0023	96	1.4286	1.7293	α CO (42) +βCCN (25)
	110	108	3.369	3.2303	108	1.8842	3.3645	τ SO_2 (47)
		123	0.1256	1.5302	122	1.4073	7.3619	α C N (38)
	137	135	1.7866	1.2223	134	0.9822	5.0767	γCH (14)
	159	156	0.2621	2.4941	157	1.4147	0.3074	τCH_3 (61)
	165	165	0.5156	4.7382	165	3.3576	7.4599	β C N (37)
		177	1.9767	1.8281	177	1.14	1.8434	τring 1 (50)
	198	197	5.8575	6.0326	198	0.6931	5.7517	τCH_3 (46)
	210	208	3.0712	3.385	210	3.8666	6.8132	βNCC(15) + γCH (12)
		215	5.7818	2.5539	216	3.2726	0.5652	τCH_2 (54)
	239	238	0.688	6.8917	237	3.902	6.9165	βCCC(23)
	250	249	3.243	8.2459	250	1.4803	0.3009	βring(29)
	275	276	1.3283	1.0886	273	1.4059	3.0146	νCC(33) + γring 1 (52)
		285	5.1125	3.0074	288	0.0108	1.2474	τring (11)+ βCCC (21)
		297	4.6406	2.0371	297	7.5612	3.0436	γCN (13)
	310	310	5.2285	4.1576	310	0.5201	17.9793	βring (10)
		322	11.9369	1.8695	320	35.2436	0.9348	γCBr (24)
	335	336	0.4738	3.8042	335	15.2092	1.8394	τring(17)+ βNCH(14)
	367	362	10.5417	5.699	365	2.2389	4.4095	δring 4 (56)
	391	389	1.3799	3.5916	390	36.2004	0.2192	γring 4 (53) + γCS (45)
410		409	6.8595	3.043	410	58.818	8.5086	τ ring (18) +γCH(15)
	415	414	0.2318	0.429	415	94.5433	63.6479	β Ring (21)
437		437	5.4654	2.4904	435	17.3606	18.7207	γCN (68)
460		459	33.7023	3.9011	457	12.6489	1.0269	γCN (13)
470		469	14.2091	3.2418	469	43.4779	134.8462	γring 4 (27)
	477	479	41.9241	0.9477	477	3.0205	1.7523	δNS (63)
485	486	485	36.0777	1.7802	488	30.3755	1.8544	δring 4 (21)
541	541	541	10.2323	3.3707	540	127.1302	47.155	τNC(11) +βCCO(25)
556	557	555	72.1051	2.4059	554	85.9678	116.8706	βring (22)
	575	573	330.3519	19.8844	569	286.8296	28.5812	γCH(17)+ γCN(13)
583		581	7.8655	1.1436	581	135.6455	9.0546	νCS (65)
601		601	5.1811	1.7432	603	48.9739	125.2522	γCO(35)+τNC(18)

614	614	614	11.5968	6.5275	613	33.1744	501.7748	γNH (34)
627		625	1.2332	5.0249	622	5.6628	4.7	νCBr(47)
	630	629	10.0151	1.532	627	12.7616	194.8099	γCC(21)
648	648	647	1.0679	3.5545	648	0.3751	82.3409	γCN(32)
669		667	12.0609	7.1027	670	11.7727	73.4867	βCCN(21)
703		700	27.6541	0.1272	701	266.8136	121.5203	βNCH(29)
710		705	6.4823	17.3033	709	29.4214	58.1269	γCC(18)
721	722	721	20.6485	4.0236	723	66.3957	171.7569	γCH(23)
730		729	49.3904	0.9791	731	91.8194	32.1415	νCS (66)
754		753	44.3583	4.837	757	21.4717	1.2795	βring(13)
	765	762	52.8016	2.1941	765	129.5173	0.1488	γCH(48)+γCN(9)
770		769	18.8524	4.2745	770	13.612	0.4494	γCH (54)
781		779	2.8786	1.5645	781	50.0521	9.9843	νCC(23)
810	810	808	88.0053	25.7125	807	35.4862	4.7211	γCH(79)
857	857	857	5.1239	7.1573	860	2.998	1.5771	γCN(16)+ βNCH(14)
866		864	1.1673	3.8844	866	286.0304	2.961	γCC(31)+ τring(12)
	873	872	21.0865	32.0957	873	12.0052	0.237	γSO(49)
881	881	882	0.3154	4.1545	881	36.1403	0.6428	γSO(45)
895		892	10.3369	12.1979	896	13.7845	0.9494	νCN(23)
913	913	914	46.0237	2.149	916	23.4539	0.6046	νCC(65)
939	939	938	0.8254	0.7775	939	11.1309	1.1773	γCN(24)
962	963	962	1.6116	0.5497	962	5.3671	5.3797	γCH(42)
984	982	981	1.2565	1.0896	981	0.2849	7.0499	γCC(11)
996		993	140.8646	61.1145	995	1.1122	0.9627	γCH(29)
1002		1000	1.4465	0.5973	1002	2.5017	1.3859	νCC(67)
	1005	1002	9.9521	3.2241	1005	102.5242	3.1266	νCN(35)
1013		1012	15.9355	14.5358	1014	3.2828	55.4191	γCO(14)
1019	1020	1020	0.4876	0.5748	1019	61.7769	0.9226	βCCH(9)
1035		1034	26.4261	12.4803	1036	21.3977	3.9826	γCH(37)+ βCCC(29)
1042	1043	1042	26.4904	79.8331	1041	11.1439	19.6073	νCC(69)
	1047	1047	2.711	24.4658	1047	137.3954	4.2351	τring(11)
1060		1059	8.3837	1.031	1059	20.5565	5.292	βCCH(41)
	1062	1061	22.6545	21.7123	1061	103.3909	8.8231	νCC(71)
1083		1083	102.7628	7.0954	1083	5.6552	29.3357	βNCH(16)+ βring(21)
1088		1085	43.9156	24.141	1086	21.6893	35.2166	δSO (30)
1105	1105	1104	20.1372	6.8336	1104	7.0952	8.3466	βCCH(16)+ βring(11)
1118		1117	5.5867	0.7179	1118	3.3194	40.6016	βNCH(27)+ βCCH(17)
1139	1140	1139	28.6267	5.6918	1139	2.1542	167.504	νCC(53)
1152		1152	163.3947	35.4004	1153	9.8207	0.1879	νCN(61)
1180	1180	1179	1.5993	7.6944	1180	2.0218	0.1817	βCCH(26)
1189		1187	14.7777	13.9748	1188	49.2618	11.6157	νCC(52)
1193	1192	1191	19.3232	6.4501	1193	1.7645	16.4284	βCCH(22)
1203		1201	3.4755	4.4635	1203	0.5752	2.8527	βCCH(23)
1210	1210	1209	35.2171	23.645	1210	9.5028	31.3909	νCC(65)
1217		1215	4.2444	8.8588	1216	16.2375	12.9365	ν_sSO (73)
1236		1235	269.3375	141.1366	1235	14.6619	80.2658	δCH (57)
1251		1250	62.7235	50.2921	1252	91.5214	113.306	βCCH(23)+βCCO(18)
1278		1276	87.9192	8.5872	1278	7.1257	5.5391	βCCH(41)+ βCCC(14)
1289	1289	1287	171.1515	79.5245	1288	53.5721	17.8528	βNCH(38)
1297		1295	574.2697	291.8097	1296	42.0132	13.7123	νCN(51)
1312	1312	1312	84.3338	30.5065	1312	0.4535	65.4806	νCC (83)
1332	1331	1329	10.1531	15.5405	1331	5.3186	521.5473	ν_aSO(69)
1347	1349	1346	18.3491	34.6359	1349	4.7912	31.7044	βCCH(83)
1353		1352	1.0577	0.6609	1351	18.4244	42.6735	νCN(41)
1358	1358	1356	93.9758	2.7421	1358	10.2891	152.5953	νCN(45)
1370		1369	0.5462	1.442	1370	21.3205	567.0388	βCCC(21)
	1386	1386	33.0314	13.489	1386	19.5422	54.2821	νCN(83)
1400	1400	1399	17.5413	61.7931	1400	26.2555	0.0034	νCC(77) + βCCH(41)
1415		1413	18.5558	22.8527	1415	54.4856	0.1103	νCN(66) + βHCH(49)
1428	1429	1427	82.943	175.8708	1425	4.0477	2.3257	νCC(62) + βCCH(13)
1480		1479	60.6619	26.4889	1480	44.7661	9.019	νCC(64) + βHCH(58)
	1482	1481	22.18	13.5596	1483	152.9896	0.0107	βCCC(19) + βHCH(60)
1485		1484	1.746	7.2638	1485	61.5408	15.5252	νCC(52)
	1487	1488	24.6023	3.9045	1488	318.744	0.3009	νCN(57)+ βCCC(28)
1489		1489	17.0556	23.3638	1489	344.173	0.2883	νCN(61)
1495	1495	1494	5.0712	23.5915	1495	146.1903	0.2342	νCC (73)+ βHCH(21)
1503		1502	16.068	13.6423	1503	42.7447	2.0073	νCC(56) + βCCC(23)
1512	1512	1512	7.2666	23.3171	1512	66.5497	0.251	νCC(65) + βCCH(39)
1523		1521	10.8986	49.5644	1522	20.5202	2.9124	βCCH(22)
1525		1524	3.6225	0.5131	1524	294.7853	0.0001	βCCH(43)
1557	1557	1560	195.4561	81.8822	1556	9.428	1.2642	βCCH(47)

1571	1572	1570	81.4516	320.166	1567	16.6217	5.1885	βCCH(59) + νCC(73)
1578	1575	1575	3.6331	17.7878	1576	17.5191	3.2742	βCCH(18) + νCC(76)
1583		1582	3.3792	43.4974	1582	90.1702	3.1956	βHCH(29) + βNCH(13)
1591		1590	0.7471	7.6328	1589	14.9313	3.105	νCC(73)
1598	1598	1597	19.2612	74.5746	1597	1.6016	10.5337	νCN(91)
	1603	1604	175.846	1308.638	1603	204.9497	20.357	νCC(87) + βring(13)
1620		1619	308.1437	7.237	1621	294.8186	5.3885	ν CC(74) +βCCH(12)
1632		1633	395.5716	506.7204	1635	426.3753	12.6729	ν C=O(86)
2970	2970	2969	15.8759	140.2787	2966	41.1409	5.1196	ν CH(96)
3031	3030	3031	46.406	165.0253	3032	28.8077	5.769	ν CH(95)
	3045	3046	6.9456	121.037	3045	16.1647	18.2163	ν CH(97)
3067	3069	3067	21.7269	75.8576	3067	9.4172	48.227	ν_sCH(95)
3080		3078	9.284	41.372	3075	1.1268	12.1944	ν CH(97)
3091	3091	3091	9.8204	82.6357	3092	4.3978	57.0648	ν CH(96)
3127	3128	3126	7.793	46.5097	3130	5.6749	1.9686	ν CH(98)
3144		3143	14.8927	65.7899	3143	51.8132	24.0159	ν_sCH(98)
3152	3152	3152	80.8905	79.9908	3155	3.5805	2.6878	ν CH(98)
3157		3155	3.1811	69.7538	3156	12.9824	2.4214	ν CH(99)
	3159	3159	32.7902	121.5031	3160	29.231	59.3859	ν_sCH(97)
3175		3174	13.2688	183.0664	3172	57.4566	98.1889	ν CH(98)
3177	3177	3177	11.8424	130.8937	3176	22.1939	13.142	ν_{as}CH(97)
	3180	3179	10.895	36.4725	3178	14.1322	1.8912	ν CH(99)
3183	3183	3182	19.7125	230.6675	3182	20.0416	7.0843	ν_{as}CH(99)
3187		3186	9.9424	58.8921	3187	60.0427	30.4279	ν_{as}CH(99)
3190	3190	3189	2.714	84.829	3188	89.373	4.2871	ν_{as}CH(98)
	3198	3197	3.8723	51.7064	3195	49.7519	15.5592	ν_{as}CH(99)
3220	3221	3221	2.8736	86.0055	3217	53.9112	13.0634	ν_{as}CH(98)
3473	3475	3476	28.0929	48.9317	3481	65.0711	10.1653	ν NH(99)

Table 3 The calculated μ, α and βcomponents of M32A1PI3P

Parameters	B3LYP/ 6-31G(d,p)	B3LYP/ 6-311++G(d,p)	Parameters	B3LYP/ 6-31G(d,p)	B3LYP/ 6-311++G(d,p)
μ_x	0.2324	0.2156	β_{xxx}	651.051	437.462
μ_y	-1.8246	0.4167	β_{xxy}	-128.552	-98.241
μ_z	-1.4842	1.2380	β_{xyy}	112.753	87.108
μ	2.3634	2.7377	β_{yyy}	44.593	-67.407
α_{xx}	376.244	316.158	β_{xxz}	-95.929	82.838
α_{xy}	13.362	16.775	β_{xyz}	74.482	31.205
α_{yy}	274.234	219.741	β_{yyz}	-80.356	54.525
α_{xz}	-4.332	6.643	β_{xzz}	17.593	9.969
α_{yz}	-13.581	-23.783	β_{yzz}	-22.031	18. 601
α_{zz}	184.754	188.310	β_{zzz}	-11.631	-13.581
α_{tot}	278.411	241.403	β_{tot}(esu)	1.789×10^{-30}	1.816×10^{-30}
Δα	672.574	560.432			

Table 4 Molecular properties of M32A1PI3P

Molecular properties	B3LYP 6-31G(d,p)	B3LYP 6-311++G(d,p)	Molecular properties	B3LYP 6-31G(d,p)	B3LYP 6-311++G(d,p)
E_{HOMO} (eV)	-5.8567	-8.7934	Chemical hardness (η)	2.0663	3.8918
E_{LUMO} (eV)	-1.7241	-1.0098	Softness (S)	0.4839	0.2569
$E_{HOMO-LUMO}$ gap (eV)	4.1326	7.7836	Chemical potential (μ)	-3.7904	-4.9016
Ionisation potential (I) eV	5.8567	8.7934	Electronegativity (χ)	3.7904	4.9016
Electron affinity(A) eV	1.7241	1.0098	Electrophilicity index (ω)	7.1835	12.0128

Table 5 Occupancy, percentage of p character of significant natural atomic hybrid of the natural bond orbital, Significant of NLMO's of M32A1PI3P calculated at B3LYP/6-311++ G(d,p)

Donor	Accepot	E(2)[a] Kj/mol	Hybrid	ED(e)	%from Parent NBO	Hybrid Atom	Cont atom	Atom	percentage
π C_{21}-C_{22}	π*C_{18} - C_{23}	26.06	$P^{1.00}$	1.72935	80.456	C_{18},C_{23}	19.28	C_{21}-C_{22}	99.99
LP (2) O_4	σ *C_1 -O_5	36.83	$P^{1.00}$	1.98817	92.459	C_1,O_5	6.139	O_4	99.99
LP (2) O_5	σ * C_1 –O_4	47.60	$P^{1.00}$	1.83184	89.840	C_1,O_4	8.966	O_5	99.99
LP (1)N_6	π * C_7 - C_8	30.60	$P^{1.00}$	1.85330	82.094	C_7,C_8	13.74	N_6	99.98
LP (3) O_{16}	σ *N_6 - S_{15}	38.31	$P^{1.00}$	1.91176	88.279	N_6,S_{15}	10.10	O_{16}	99.99
LP (3) O_{17}	σ *N_6 - S_{15}	35.28	$P^{1.00}$	1.95446	89.365	O_{16},S_{15}	10.01	O_{17}	99.99
LP (2) O_{27}	σ *C_{25} - N_{28}	22.83	$P^{1.00}$	1.93267	93.390	C_{26},C_{25}	5.597	O_{27}	99.99
LP (1) N_{28}	π * C_{25} - O_{27}	52.67	$P^{1.00}$	1.78935	84.638	C25, O_{27}	13.69	N_{28}	99.99

Table 6 Mullikan atomic charges table of M32A1PI3P

Atom	B3LYP/ 6-31G(d,p)	B3LYP/ 6-311++G(d,p)	Atom	B3LYP/ 6-31G(d,p)	B3LYP/ 6-311++G(d,p)
C	0.61243	0.61356	C	-0.39084	-0.39110
C	-0.16534	-0.16673	O	-0.50872	-0.50901
C	-0.10971	-0.10768	N	-0.51245	-0.51202
O	-0.49110	-0.49673	C	-0.08105	-0.08149
O	-0.49341	-0.49162	H	0.11761	0.11093
C	-0.79940	-0.80024	H	0.10258	0.10808
C	0.29771	0.29996	H	0.09616	0.09514
C	0.02061	0.01881	H	0.09295	0.08802
C	0.05995	0.05985	H	0.09161	0.08878
C	-0.13870	-0.13885	H	0.10837	0.10950
C	-0.09357	-0.09361	H	0.17111	0.17252
C	-0.10890	-0.10910	H	0.11704	0.11133
C	-0.07078	-0.07050	H	0.11119	0.10259
C	0.28658	0.28737	H	0.10659	0.10370
S	1.29582	1.30043	H	0.13159	0.13593
O	-0.53473	-0.52993	H	0.18944	0.19186
O	-0.53181	-0.52610	H	0.13133	0.14032
C	-0.19021	-0.18990	H	0.10610	0.10685
C	-0.07878	-0.07811	H	0.15757	0.14916
C	-0.09760	-0.09781	H	0.14987	0.15058
C	-0.07118	-0.07152	H	0.26580	0.26569
C	-0.08630	-0.08640	H	0.10865	0.11501
C	-0.08296	-0.08235			

Table 7 Thermo dynamical properties of M32A1PI3P

T (K)	S (J/mol.K)		Cp (J/mol.K)		ddH (kJ/mol)	
100	470.02	418.24	194.06	156.55	12.08	9.92
200	641.55	557.97	313.98	258.4	37.51	30.66
298.15	789.16	680.3	433.6	361.47	74.19	61.07
300	791.85	682.54	435.84	363.41	74.99	61.74
400	933.41	801.04	551.65	463.25	124.48	103.17
500	1067.49	913.87	650.58	548.51	184.75	153.89
600	1193.49	1020.24	731.13	617.94	253.98	212.34
700	1311.26	1119.87	796.32	674.18	330.46	277.04
800	1421.19	1213	849.63	720.28	412.85	346.84
900	1523.89	1300.11	893.86	758.59	500.09	420.84
1000	1620.04	1381.76	930.97	790.81	591.38	498.35

CONCLUSION

Density functional theory calculations were calculated for a complete structural, thermodynamic, first-order hyperpolarizability, Mulliken population analysis, vibrational and electronic investigations of M32A1PI3P. The gas phase structure and conformational properties of M32A1PI3P were determined by quantum chemical calculations. The equilibrium geometries and harmonic frequencies of M32A1PI3P were determined and analyzed at the DFT level utilizing B3LYP/6-31G(d,p) and B3LYP/6-311++G(d,p) basis set, giving allowance for the lone pairs through diffuse functions. The difference between observed and calculated wavenumber values of the most of the fundamental modes is very small. The calculated first order hyperpolarisability is found to be 1.816 x 10^{-30} e.s.u. The various intramolecular interactions that are responsible for the stabilization of the molecule was revealed by the natural bond orbital analysis. The energies of HOMO & LUMO and their orbital energy gaps are calculated using B3LYP/6-311++G(d,p) method which provide the nature ofreactivity. The frontier orbital energy gap (E_{HOMO} - E_{LUMO}) isfound to be 7.7836 eV. Thus the present inves- tigation furnishes the complete vibrational assignments, structural information and electronic details of the compound .

REFERENCES

[1] Joshi K.C, Chand.P, *Pharmazie*, **1982**, 37, 1–12.
[2] Pomarnacka .E, Kozlarska-Kedra .I, *Farmaco*, **2003**, 58, 423–429.
[3] Quetin-Leclercq .J, J. Pharm. Belg., **1994**, 49, 181–192.
[4] Mukhopadhyay.S, Handy G.A., Funayama .S, Cordell G.A., *J. Nat.Prod*., **1981**, 44, 696 – 700.
[5] Gunasekaran .B , Radhakrishnan Sureshbabu, Mohanakrishnan A.K., Chakkaravarthi G, Manivannan .V, *Acta Cryst.*, **2009**, E65, o1856.
[6] Chakkaravarthi .G, Sureshbabu .R, Mohanakrishnan A.K., Manivannan V, **2008**, *Acta Cryst*. E64, o732.
[7] Chakkaravarthi .G, Dhayalan .V, Mohanakrishnan A.K., Manivannan .V, **2007**, *Acta Cryst*. E63, o3698.

[8] Frisch M.J, Trucks G.W, Schlegel H.B, Scuseria G.E, Robb M.A, Cheeseman J.R, Montgomery J.A Jr., Vreven T, Kudin K.N, Burant J.C, Millam J.M, Iyengar S.S, Tomasi .J, Barone V, Mennucci B, Cossi .M, Scalmani .G, Rega .N, Petersson G.A, Nakatsuji .H, Hada .M, Ehara .M, Toyota .K, Fukuda .R, Hasegawa .J, Ishida .M, Nakajima .T, Honda .Y, Kitao .O, Nakai .H, Klene .M, Li .X, Knox J.E, Hratchian H.P., Cross J.B, Bakken .V, Adamo .C, Jaramillo .J, Gomperts .R, Stratmann R.E, Yazyev .O, Austin .A.J, Cammi .R, Pomelli .C, Ochterski .J.W, Ayala P.Y, Morokuma.K, Voth G.A, Salvador .P, Dannenberg J.J., Zakrzewski V.G., Dapprich S, Daniels A.D, Strain M.C, Farkas O, Malick D.K, Rabuck A.D, Raghavachari K, Foresman J.B, Ortiz J.V, Cui.Q, Baboul A.G, Clifford .S, Cioslowski .J, Stefanov B.B, Liu .G, Liashenko .A, Piskorz .P, Komaromi .I, Martin R.L, Fox D.J, Keith .T, Al- Laham M.A, Peng C.Y, Nanayakkara .A, Challacombe .M, Gill P.M.W, Johnson .B, Chen .W, Wong M.W, Gonzalez .C, Pople J.A, Gaussian 03W Program, Gaussian Inc., Wallingford, CT, **2004**.
[9] Becke A.D., *J. Chem. Phys*. 98, **1993**, 5648–5652.
[10] Lee C., Yang .W, Parr R.G., *Phys. Rev*. B37, **1988**, 785–789.
[11] Fogarasi G, Pulay P, Durig J.R. (Eds.), *Vibrational Spectra and Structure*, vol. 14, Elsevier, Amsterdam, **1985**, pp. 125 (Chapter 3).
[12] Fogarasi G, Zhou X, Taylor P.W, Pulay P, *J. Am. Chem. Soc*. 114, **1992**, 8191–8201.
[13] Sundius .T, *J. Mol. Struct*. 218, **1990**, 321–326.
[14] Sundius .T, *Vib. Spectrosc*. 29, **2002**, 89–95.
[15] MOLVIB (V.7.0): Calculation of Harmonic Force Fields and Vibrational Modes of Molecules, QCPE Program No. 807, **2002**.
[16] Frisch .A, Nielson A.B, Holder A.J, Gaussview Users Manual, Gaussian Inc., Pittsburgh, PA, **2000**.
[17] Silverstein M, Bassler G.C, Morril C, Spectroscopic Identification of Organic Compounds, John Wiley, Newyork, **1981**.
[18] Arjunan .T, Rani C.V, Mythili.S, Mohan.S, *Spectrochim. Acta* 79A, **2011**, 486–496.
[19] Rajamani.T , Muthu.S , Karabacak .M, *Spectrochim. Acta* 108A, **2013**, 186–196.
[20] Socrates .G, Infrared and Raman Characteristic Group Frequencies—Tables and Charts, third ed., Wiley, New York, 2001.
[21] Gunasekaran .S, Seshadri.S, Muthu.S, Kumaresan.S, Arunbalaji .R, *Spectrochim. Acta* A 70, **2008**, 550-556.
[22] Mohan .J, Organic Spectroscopy—Principle and Applications, 2nd ed., Narosa Publishing House, New Delhi, **2004**, pp. 30
[23] Puviarasan.N, Arjunan.V, Mohan.S, *Turk. J. Chem*. 26, **2002**, 323–334.
[24]Varsanyi .G, Assignments for Vibrational spectra of Seven Hundred Benzene derivatives, ½ Academic Kiaclo, Budapest, **1973**.
[25] Krishnakumar .V, John Xavier .R, *Indian J. Pure Appl. Phys*. 41, **2003**, 597–602.
[26] Krishnakumar .V, Prabavathi V.N, *Spectrochim. Acta, Part A 71*, **2008**, 449 – 457.
[27] Silverstein .M, Clayton Basseler G, Morill .C, Spectrometric identification of Organic compounds, Wiley, New York, **1981**
[28] Chitambarathanu .T, Umayourbaghan .V, Krishnakumar .V, *Indian J. Pure & Appl. Phys*., 41, **2003**, 844-849.
[29] Gunasekaran .S, Natarajan R.K, Rathika .R, Syamala D, *Ind .J. Phys*. 79, **2005**, 509- 515.
[30] Lakshamaiah .B, Ramana Rao .G, *J. Raman Spectrosc*, 20, **1989**, 439-445
[31] Bellemy L.J, The Infrared spectra of complex molecules, John Wiley, New York, **1956**.
[32] Mohan .S, Ilangovan.V, *Indian J. Pure & Appl. Phys*., 32, **1994**, 91-96
[33] Singh D.N, Singh I.D, Yadav R.A, *Indian J. Phys*., 76B(1), **2002**, 35-41
[34] Venkataramana Rao .P, Ramana Rao.G, *Spectrochim Acta Part A*, 59, **2003**, 637
[35] Gunasekaran .S, Ponnambalam.U, Muthu .S, Mariappan .L, *Asian J. Phys*.,**2003**,16,1,51.
[36] Roggers P.G , A guide to the complete interpretation of Infrared spectra of organic structures, Wiley, Canada, **1994**.
[37] Seshadri .S, Gunasekaran .S, Muthu .S, *J. Raman Spec*, 40, **2009**, 639-644.
[38] Jong Rack Sohn, Won Cheon Park, *Bull. Korean Chem. Soc*., 22,12, **2001**, 1297-1298.
[39] Kleinman D.A, *Phys. Rev*. 126, **1962**, **1977**.
[40] Koopmans T.C, *Physica* (Amsterdam) 1, **1933**, 104.
[41] Ebenso E.E, Arslan .T, Kandemirli .F, Love .I, Ogˇretir .C, Saracogˇlu .M, Umoren S.A., *Int. J. Quantum Chem*. 110, **2010**, 2614.
[42] O' Boyle N.M, Tenderholt A.L, Langer K.M, *J. Comput. Chem*. 29, **2008**, 839–845.
[43] Parr R.G, Szentpaly .L, Liu .S, *J. Am. Chem. Soc*. 121, **1999**, 1922–1924.
[44] Parthasarathi .R, Padmanabhan .J, Elango M, Subramanian V, Chattaraj P, *Chem. Phys. Lett*. 394, **2004**, 225–230.
[45] Parthasarathi .R, Padmanabhan .J, Subramanian .V, Maiti .B, Chattaraj .P, *Curr.Sci*. 86, **2004**, 535–542.
[46] Parthasarathi .R, Padmanabhan .J, Subramanian .V, Sarkar .U, Maiti .B, Chattaraj .B, *Internet Electron. J. Mol. Des*. 2, **2003**, 798–813.
[47] Thomson H.W, Torkington .P, *J. Chem. Soc*. 171, **1945**, 640-646.

[48] Glendening E.D, Badenhoop J.K, Reed A.E, Carpenter J.E, Bohmann J.A., Morales C.M , Weinhold F., NBO 5.0, Theoretical Chemistry Institute, University of Wisconsin, Madison, **2001**.
[49] Reed A.E, Curtiss L.A, Weinhold F, *Chem. Rev*. 88, **1988**, 899–926.
[50] Reed A.E, Schleye P.V.R, *Inorg. Chem*. 27, **1988**, 3969–3987.
[51] Xavier R.J, Gobinath .E, *Spectrochim. Acta* A 91, **2012**, 248–255.
[52] Politzer .P, Murray J.S., Theoretical biochemistry and molecular biophysics: acomprehensive survey, in: D.L. Beveridge, R. Lavery (Eds.), ElectrostaticPotential Analysis of Dibenzo-p-dioxin and Structurally Similar Systems inRelation to Their Biological Activities, Protein, vol. 2, Adenine Press, Schenectady, NY, **1991** (Chapter 13).
[53] Politzer P, Laurence P.R, Jayasuriya .K, Molecular electrostatic potentials: an effective tool for the elucidation of biochemical phenomena, in: J. McKinney (Ed.), Structure Activity Correlation in Mechanism Studies and Predictive Toxicology, *Environ. Health Perspect*, vol. 61, **1985**, pp. 191–202.
[54] Okulik N, Jubert A.H, *Internet Electron, J. Mol. Des*. 4, **2005**, 17–30.
[55] Irikura K.K, THERMO.PERL Script, National Institute of Standards and Technology **2002**.